Catalysis Today 143 (2009) 137–144

Contents lists available at ScienceDirect

Catalysis Today

journal homepage: www.elsevier.com/locate/cattod

# Al-SBA-15 as a support of catalysts based on chromium sulfide for sulfur removal

M. Gómez-Cazalilla, A. Infantes-Molina, R. Moreno-Tost, P.J. Maireles-Torres,
J. Mérida-Robles, E. Rodríguez-Castellón, A. Jiménez-López [*]

*Departamento de Química Inorgánica, Cristalografía y Mineralogía (Unidad Asociada al ICP-CSIC), Facultad de Ciencias,*
*Universidad de Málaga, Campus de Teatinos, 29071 Málaga, Spain*

ARTICLE INFO

*Article history:*
Available online 27 September 2008

*Keywords:*
Mesoporous SBA-15
Chromium sulfide
Dibenzothiophene
HDS

ABSTRACT

SBA-15 doped with aluminium supported Cr catalysts were prepared with different chromium contents by the wetness impregnation method. The materials in oxidic and sulfided states were characterized by X-ray diffraction (XRD), $N_2$ adsorption–desorption isotherms at 77K, $NH_3$-TPD, XPS analysis and $H_2$-TPRS. The catalytic properties of these materials with the hydrodesulfurization (HDS) of dibenzothiophene (DBT) were tested at 260–340 °C under a hydrogen pressure of 3.0 MPa. The catalytic behaviour was studied as a function of the Cr loading and the support. A mesoporous silica (SBA-15) was also used to prepare the Cr catalysts in order to study the influence of the support on the catalytic performance. The catalyst based on SBA-15 showed very low catalytic activity in the reaction conditions studied whereas the AlSBA-15 based catalyst showed very good performance in hydrotreating, depending on the Cr loading. These results suggest that catalytic activity, which is directly related to the amount of labile sulfur, can vary not only as a function of the Cr content, but also with the incorporation of aluminium to the mesoporous silica. This highly modifies the nature of the acidic properties of the support, providing a stronger metal–support interaction, allowing better dispersion of the chromium species and specific electronic properties of the active species that affect the catalyst performance.

## 1. Introduction

In the past decade, clean fuels research, including desulfurization, has grown in importance as a subject in worldwide environmental catalysis studies. The issues of gasoline and diesel deep desulfurization are becoming more serious due to crude oils becoming higher in sulfur content and heavier in density, while the regulation sulfur limits are becoming lower and lower. The challenges for catalysts suppliers is to provide increased hydrodesulfurization (HDS) activity, required to meet specific targets for ultra low sulfur diesel markets (less than 10 ppm sulfur by 2010), while hydrotreating ever heavier petroleum feeds [1,2]. Thus, the development of highly active and selective HDS catalysts is one of the most important concerns that the petroleum industry has to face at present.

The basic composition of current hydrotreating catalysts is a molybdenum or tungsten sulfide, promoted by cobalt or nickel as active phases, and mainly porous γ-alumina as a material support. While considerable progress has been achieved by improving the properties of these sulfide systems, the nature of the active phase has hardly been modified in decades [3,4]. However, by changing the support material [5] by adding additives (e.g., boron or phosphorus or silica) or promoters to the catalyst, as well as by changing the preparation method used, a noticeable alteration in the catalyst performance is achieved. Nonetheless, currently there is no doubt that the nature of the active phase remains the same, i.e. slabs of $Mo(W)S_2$ which are edge-decorated with cobalt or nickel. Against molybdenum and tungsten, the another transition metal of group 6, chromium, have only been used in a few cases in the HDS processes [6]. The use of chromium catalysts will greatly reduce the expense of HDS processes because of the low cost of chromium. Chromium is also a relatively small atom which can be loaded on supports in high proportions to achieve better catalytic activities without causing problems of dispersion. According to the literature, it seems that the inherent activity is between those of molybdenum and tungsten and is dependent on the support and the preparation method used. It is also well known that by increasing the active metal loading and adding a proper promoter,

---

[*] Corresponding author. Tel.: +34 952131876; fax: +34 952137534.
*E-mail address:* ajimenezl@uma.es (A. Jiménez-López).

0920-5861/$ – see front matter © 2008 Elsevier B.V. All rights reserved.
doi:10.1016/j.cattod.2008.07.035

the catalytic activity for HDS and HDN can be greatly improved. In particular, the use of $Cr/Al_2O_3$ [7], Cr-exchanged zeolites [8], carbon-supported chromium catalysts [9], and Cr-pillared clays [10,11] have been studied. More recently, Kabe and co-workers [12] have studied the catalytic activity in the HDS of DBT of Cr, CrCu, CrNi and CrCo alumina supported catalysts and they showed that the activity is directly correlated with the amount of labile sulfur in the surface, i.e. the weaker the chromium–sulfur bond the higher the number of labile sulfur atoms, thus leading to an increase in the number of active sites. Sulfidation temperature also seems to play a very important role on catalytic activity since the species present on the catalyst surface can vary composition in a wide range. With reference to this, Kabe and co-workers [13] have studied the sulfidation process of $CrO_3$ supported on $Al_2O_3$ by using different temperatures and sulfidation procedures obtaining different $CrS_x$ species and percentages of sulfidation. Pakkanen and co-workers [14] studied the catalytic activity of CrCo supported on alumina in thiophene hydrodesulfurization. These authors found the best catalytic results in HDS when the bimetallic CrCo/alumina was reduced before the sulfidation step, so long as the highest sulfur/metal ratio was obtained. These results indicate that different CrCoS phases were formed when the bimetallic CrCo/alumina system was reduced before the sulfidation step.

On the other hand, in order to obtain more active HDS catalysts, many approaches have been followed, with the variation of the support being an important one. The support effect in the HDS reaction has been analysed in detail in recent reviews [5,15]. Different materials have been tested as supports to study its role on the dispersion of the active phase and promoters as well as the metal–support interaction influence on the catalytic activity [5,15–17]. The commercial HDS catalysts use $\gamma$-$Al_2O_3$ as a support, but many other supports have been studied including zeolites such as Y, USY and mesoporous materials such as MCM-41 [18,19], HMS [20,21], SBA-15 [22–24] and mesoporous $Al_2O_3$ [25]. The potential advantage of mesoporous hosts for the preparation of catalytic phase materials lies in the high dispersion of the catalytic phase at high loadings. As regards the use of SBA-15-supported catalysts for hydrotreating, there are some studies which show that this ordered mesoporous material is a suitable support to obtain high-performance catalysts in HDS reactions. Compared to HMS and MCM-41, the SBA-15 material has thicker pore walls and better hydrothermal stability, which is very important for hydrotreating processes, since these are carried out under severe reaction conditions. Thus, Vradman et al. [26] used Ni-W-S/SBA-15 catalysts and reported a higher HDS and hydrogenation activity than a commercial one such as Co-Mo/$\gamma$-$Al_2O_3$. In the same way, Murali Dhar et al. [22] showed better HDS and hydrogenation activity for Mo, CoMo and NiMo SBA-15-supported catalysts than that obtained by using $\gamma$-$Al_2O_3$ as a support. It is also known that sulfur removal from petroleum feedstocks is enhanced to some extent by acidic sites in the surface of the catalyst. With regards to this, the same group in a later study [23] reported on Mo, CoMo and NiMo catalysts using Al-SBA-15 of various Si/Al ratios as a support for HDS and HYD purposes. They found that both SBA-15 and Al-SBA-15 supported catalysts showed similar activities for HDS, but the activity in HYD for the Al-SBA-15 support was clearly greater than that of SBA-15 due to the high molybdenum dispersion on Al-SBA-15.

Thus, in the present work the hydrodesulfurization properties of pure SBA-15 and aluminium doped SBA-15 supported chromium sulfide catalysts were examined by studying the hydrodesulfurization of dibenzothiophene (DBT). The effect of the acidity of the mesoporous support and of the chromium content on the catalytic activity was also studied.

## 2. Experimental

### 2.1. Preparation of catalysts

The support material used to prepare chromium-based catalysts was aluminium doped mesoporous silica (Al-SBA) with a Si/Al molar ratio of 10, prepared by post-synthesis alumination, as described elsewhere [27]. The catalysts were prepared by the incipient wetness impregnation method with $Cr(NO_3)_3{\cdot}9H_2O$ as the precursor salt. First, the chromium aqueous solution was added to the pelletized support (0.85–1.00 mm), then it was air dried at 60 °C and finally, the sample was placed in tubular reactor, heated from rt to 450 °C (10 °C $min^{-1}$) and maintained for 2 h at this temperature under a $N_2$ flow (60 ml $min^{-1}$) to obtain the corresponding catalyst precursors. With this inert treatment, it is possible to avoid the formation of a high oxidation state of chromium, which can otherwise oxidize the $H_2S$ gas into sulfur during the posterior sulfidation process.

The samples were denoted as AlSBACr-*x*, where *x* is the percentage by weight of $CrO_3$.

Thus, the concentration of the precursor solutions were adjusted to the desired metal loading in each catalyst to give 15, 20, 25 and 30 wt% of $CrO_3$.

### 2.2. Characterization of catalysts

X-ray powder diffraction patterns were obtained by using a Siemens D5000 diffractometer (Cu K$\alpha$ source) provided with a graphite monochromator. Elemental Chemical Analysis was performed with a LECO CHNS 932 analyser.

Transmission electron micrographs of the samples were obtained by using a Philips CM 200 Supertwin-DX4 microscope. Samples were dispersed in ethanol. A drop of the suspension was placed on a Cu grid (300 mesh).

Hydrogen temperature-programmed reduction ($H_2$-TPRS) of the sulfided catalysts was carried out between 50 and 700 °C using a flow of 10% $H_2$/Ar (48 ml $min^{-1}$) and a heating rate of 10 °C $min^{-1}$. Prior to the analysis the precursors were sulfided in situ at 400 °C (2 h) using a flow of $H_2S/N_2$ (10/90% with a flow rate of 60 ml $min^{-1}$). Water produced in the reduction reaction was eliminated by passing the gas flow through a cold finger (−80 °C). The $H_2$-consumption was controlled by an on-line gas chromatograph (Shimadzu GC-14A) provided with a TCD.

Temperature-programmed desorption of ammonia ($NH_3$-TPD) was carried out to evaluate the total acidity of the catalysts. Catalysts were sulfided at atmospheric pressure by flowing sulfiding mixture from room temperature to 400 °C with a heating rate of 10 °C $min^{-1}$ and maintaining the sample at 400 °C for 2 h. After cleaning with helium and adsorption of ammonia at 100 °C, the $NH_3$-TPD was performed between 100 and 550 °C with a heating rate of 10 °C $min^{-1}$ by using a helium flow and maintained at 550 °C for 15 min. The evolved ammonia was analysed by on-line gas chromatography (Shimadzu GC-14A) provided with a TCD.

X-ray photoelectron spectra were collected using a Physical Electronics PHI 5700 spectrometer with non-monochromatic Al K$\alpha$ radiation (300 W, 15 kV, 1486.6 eV) with a multi-channel detector. Spectra of pelletized samples were recorded in the constant pass energy mode at 29.35 eV, using a 720 $\mu$m diameter analysis area. Charge referencing was measured against adventitious carbon (C 1s at 284.8 eV). A PHI ACCESS ESCA-V6.0 F software package was used for data acquisition and analysis. A Shirley-type background was subtracted from the signals. Recorded spectra were always fitted using Gaussian–Lorentzian curves in order to determine the binding energy of the different element core levels more accurately, except in the case of Cr 2p signals, where asymmetric curves were used.

### 2.3. Catalytic test

The hydrodesulfurization of DBT was chosen for the catalytic test, which was performed in a high-pressure fixed-bed continuous-flow stainless steel catalytic reactor (9.1 mm in diameter, and 230 mm in length), operated in the down-flow mode. The reaction temperature was measured with an interior placed thermocouple in direct contact with the catalyst bed. The organic feed consisted of a solution of DBT (1 wt%) in *n*-hexane that was supplied by means of a Gilson 307SC piston pump (model 10SC). For the activity tests, 0.5 g of catalyst was used (particle size 0.85–1.00 mm) and was diluted with quartz sand to 3 cm$^3$. Prior to the activity test, the catalysts were sulfided in situ at atmospheric pressure with a $N_2/H_2S$ (90/10%) flow of 60 ml min$^{-1}$ by heating from rt to 400 °C (2 h) at a heating rate of 10 °C min$^{-1}$. Catalytic activities were measured at different temperatures (260–340 °C), under 3.0 MPa of $H_2$, with a flow rate of 100 ml min$^{-1}$ and with hourly space velocities (WHSV) of 28 h$^{-1}$. The evolution of the reaction was studied by collecting liquid samples after 60 min at the desired reaction temperature. These liquids were kept in sealed vials for posterior analysis by gas chromatography (Shimadzu GC-14B, equipped with a flame ionization detector and a capillary column, TBR-14, coupled to an automatic Shimadzu AOC-20i injector). For these catalysts, the main products of the reaction were biphenyl (BP), cyclohexylbenzene (CHB), benzene (B) and cyclohexane (CH). For this reason, the total conversion was calculated from the ratio of converted dibenzothiophene/initial dibenzothiophene.

## 3. Results and discussion

### 3.1. Catalytic study

The catalytic performance of sulfided AlSBACr-*x* samples was tested for DBT hydrodesulfurization according to the experimental conditions described in Section 2.3. The total DBT conversions as a function of reaction temperature for the catalysts with different chromium contents are shown in Fig. 1. All catalysts show very good activity in the range of reaction temperatures studied, with conversion values at 340 °C in the range of 73.2–90.1%. The catalyst with the lowest chromium loading shows the worst data conversion, especially at low reaction temperatures. The two catalysts with the highest chromium content show very similar catalytic behaviour across the whole temperature range. The AlSBACr-20 material was the most active among the catalysts studied at all reaction temperatures. According to the literature on the Cr-based hydrotreating catalysts, species present on the surface of the catalysts can vary widely in composition as a function of the Cr content, the sulfidation temperature [13]. Hence it is reasonable to expect that the catalytic properties of each species will be different. Moreover, the activity increases when the number of labile sulfur atoms is higher. This point will be discussed in Section 3.2. A chromium catalyst with 20 wt.% of $CrO_3$ on purely siliceous SBA-15 (SBACr-20) was also studied in this catalytic reaction. A very low conversion (20%) was obtained for this material under the experimental conditions studied. This result is in accordance with previous reports [24] in which the incorporation of Ti or Zr to the SBA-15 support seems to produce changes in the dispersion of oxidic and sulfided active species that change the catalytic behaviour. Thus, the incorporation of Al onto the support surface provides a stronger metal–support interaction, allowing better dispersion of the chromium species, as will be discussed in Section 3.2.

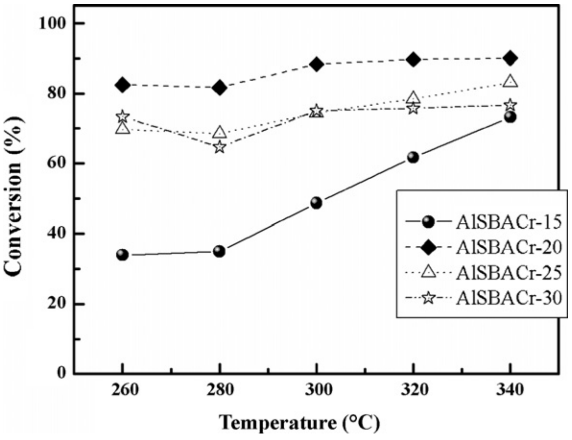

**Fig. 1.** Total DBT conversions as a function of reaction temperature for the AlSBACr-*x* catalysts. Reaction conditions: *P* = 30 bar, WHSV = 28 h$^{-1}$, $H_2$ = 100 ml min$^{-1}$.

Fig. 2 shows a comparison of the selectivities of all the catalysts at different reaction temperatures. The reaction products obtained were biphenyl (BP), cyclohexylbenzene (CHB), benzene (B) and cyclohexane (CH). Thus, taking into account Scheme 1, the HDS of DBT over these catalysts must proceed through two different pathways: direct desulfurization (DDS) to produce BP and the desulfurization of DBT prehydrogenated forming tetrahydro- and hexahydro-dibenzothiophene to produce CHB. The HYD selectivity of these chromium containing catalysts is higher than that of DDS for all catalysts across the whole temperature range. Moreover, the production of BP is seen to be practically constant with temperature change, while the selectivity to CHB decreases in the same way as the selectivity to CH increases (except for the AlSBACr-25 were the selectivity to all products is practically unchanged with the reaction temperature). It seems that the cracking of CHB is favoured at high reaction temperatures to form B and CH, and the B formed is hydrogenated to form CH. Another possibility is the hydrogenation of CHB to bicyclohexhyl (BCH), which is immediately cracked to form CH. These hydrogenation properties of the catalysts were to be expected since previous studies with chromia pillars sulfided in zirconium phosphate demonstrated that these kind of catalysts exhibit good activity for hydrogenation [11].

### 3.2. Catalyst characterization

#### 3.2.1. XRD

As a first remark, the chromium loading has been expressed as $CrO_3$ wt%, however the real state of Cr on the catalyst precursors is very likely to be $Cr_2O_3$, as the precursor catalysts display a green colour, which is characteristic of this compound. The forthcoming section will confirm this point.

X-ray powder diffraction measurements were carried out in order to identify the species formed on the samples. Fig. 3 shows the XRD patterns of the AlSBACr-*x* catalyst precursors. All the patterns show the same peaks at $2\theta = 24.5°$, 33.6°, 36.2°, 39.7°, 41.5°, 44.2°, 50.2° and 54.8°, similar to the standard pattern of $Cr_2O_3$ from the JCPDS powder diffraction file (PDF card 00-038-1479) [28]. The intensity of the $Cr_2O_3$ peaks became higher with the chromium loading. The absence of peaks in the diffractogram of the sample with the lowest Cr content (AlSBACr-15) does not exclude the presence of $Cr_2O_3$ on the surface of this sample as in the forthcoming XPS section the formation of this compound is confirmed. Due to the low loading of this sample, the formation of quite dispersed particles, not detectable by XRD, is actually expectable. On the other hand, the absence of diffraction peaks which correspond to $CrO_3$ is noticeable in the diffraction patterns of all samples. Therefore, it seems that the thermal treatment

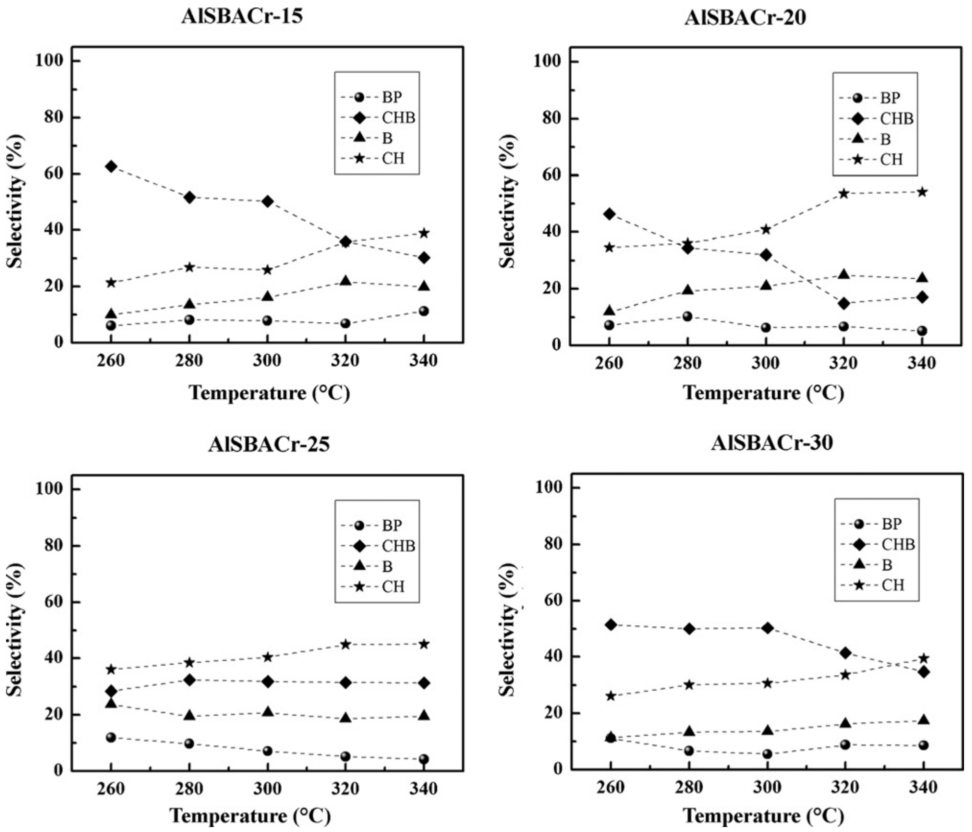

**Fig. 2.** Selectivities of DDS and HYD as a function of reaction temperature for the AlSBACr-*x* catalysts. Reaction conditions: $P = 30$ bar, WHSV = 28 $h^{-1}$, $H_2 = 100$ ml $min^{-1}$.

under nitrogen atmosphere has inhibited the oxidation of chromium(III) ions toward chromium(VI). This has been also confirmed by XPS analysis of the samples.

After the sulfidation process, the XRD patterns show the same diffraction lines due to the presence of chromium(III) oxide, which could indicate the absence of some chromium sulfide in the surface. However this fact reveals that only a partial sulfidation occurs in the surface, i.e. a superficial $Cr_xS_y$ is formed but the crystalline size of this sulfide is not big enough to be detected by this technique. Somehow, with only a superficial layer of chromium sulfide, it is enough to eliminate the sulfur atom from the dibenzothiophene (DBT) molecule, as was shown by the catalytic results.

### *3.2.2. Nitrogen adsorption–desorption isotherms at 77 K*

The surface area of the catalyst precursors were evaluated by the BET method and the corresponding results are compiled in Table 1. The surface area values corresponding to the catalyst precursors have suffered a decrease of *ca.* 50% in relation to the bare support. This decrease is greater in so far as the amount of chromium present in the system is higher. The incorporation of chromium provokes a blockage of the support porosity due to the deposition of chromium oxide particles which are larger than the support pore size. The pore volume values follow a similar trend. However, the average pore diameter of the catalyst precursor and support, calculated from the pore size distribution by using the Cranston and Inkley method for cylindrical pores, changes slightly

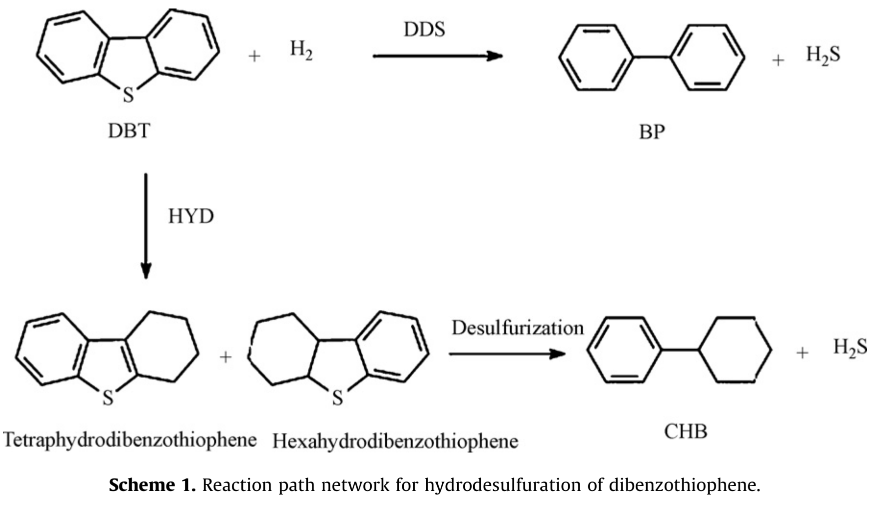

**Scheme 1.** Reaction path network for hydrodesulfuration of dibenzothiophene.

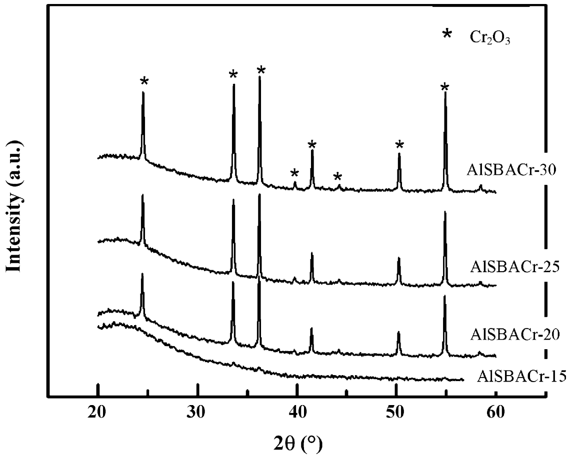

**Fig. 3.** Powder X-ray diffraction patters of AlSBACr-*x* precursors.

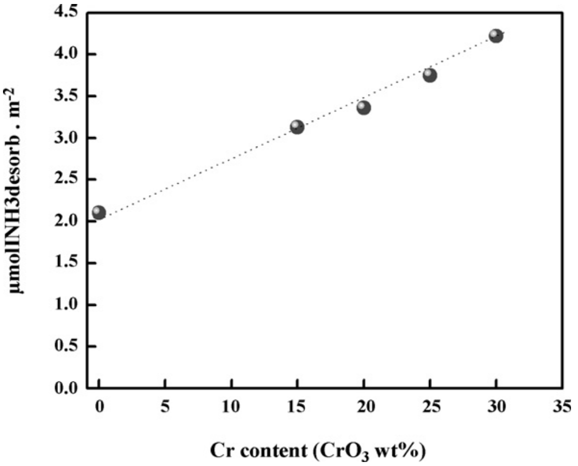

**Fig. 4.** Acidic properties of AlSBACr-*x* sulfided catalysts against chromium content.

with the chromium content. These facts are both related, with the chromium oxide particle size being the key factor to explain such behaviour. Thus, the oxide particles which posses a particle size greater than the mean pore diameter of ~180 Å, as obtained from Scherrer's equation by measuring the FWHM of the XRD patterns, are located at the external surface and cause a blockage of the pore with the concomitant decrease in surface area. For samples with a higher chromium loading, an increase in the pore diameter is observed, which is possibly due to the formation of an inherent porosity in the chromium oxide particles, as previously detected for other supported phases [29,30]. It is coherent with the pore size distribution curves (not shown), where two maxima are noticeable. Similarly, Zhang et al. [31] in an study about the properties of $CrO_x$/SBA-15 materials have also observed the appearance of a weak peak in the pore size distribution which was ascribed to a change in the $CrO_x$ particle morphology and pore shape with increasing chromium loadings.

### 3.2.3. $NH_3$-TPD

The acidic properties of this family of sulfided catalysts, as determined by the amount of $NH_3$ irreversibly adsorbed at 100 °C, is plotted as a function of the chromium content in Fig. 4. As can be clearly observed that when comparing the acidity to the surface area, it is directly related to the chromium content, and increases almost linearly with the $CrO_3$ content, including the pristine Al-SBA material support. Hence the acidity value increases gently when higher chromium oxide loadings are added to the catalyst. In all cases the acidity values of these samples are higher than that of the support (2.1 µmol $NH_3$ $m^{-2}$) The acidic properties obtained by the presence of $Cr^{n+}$ ions in the catalysts, has been previously reported by other authors [36], who have pointed out that $Cr^{3+}$ and $Cr^{6+}$ species, existing on the surface of catalysts, were responsible for the formation of strong acid sites which are highly active in cracking reactions. As the samples were sulfided previous to the ammonia adsorption, the chromium sulfide itself acts as an acid site due to the existence of some coordinatively unsaturated centres in the chromium ions. The low acidity of the pristine SBA-15 (0.27 µmol $NH_3$ $m^{-2}$) may be responsible for the low dispersion of the active phase, and as a consequence, its low activity on the HDS reaction.

**Table 1**
Textural properties of the support and the precursor catalysts

| Sample | $S_{BET}$ ($m^2$ $g^{-1}$) | $\upsilon_p$[a] ($cm^3$ $g^{-1}$) | $d_p$[b] (av) (Å) |
|---|---|---|---|
| AlSBA | 359 | 0.354 | 39.4 |
| AlSBACr-15 | 158 | 0.128 | 32.5 |
| AlSBACr-20 | 149 | 0.137 | 36.7 |
| AlSBACr-25 | 147 | 0.133 | 36.2 |
| AlSBACr-30 | 135 | 0.136 | 40.3 |

[a] $\upsilon_p$ at $P/P_0$ = 0.95.
[b] Calculated by BJH method.

### 3.2.4. XPS

The oxidation states of the elements present in the samples were further investigated by using XPS. Table 2 compiles Cr $2p_{3/2}$ and S $2p_{3/2}$ binding energy values for the catalyst precursors and sulfided catalysts. The increase of chromium loading in the catalyst precursors hardly modifies the binding energy values of the Cr $2p_{3/2}$ and S $2p_{3/2}$ signals. The Cr 2p core level spectrum for the AlSBACr-20 sample (Fig. 5), considered as representative of these systems, has been studied by an appropriate curve fitting. The spectra of chromium species, represented by the Cr 2p core level, always produced two peaks which were ascribed to the doublet Cr $2p_{3/2}$ and Cr $2p_{1/2}$. With regard to this, the spectrum of the catalyst precursor (Fig. 5A) possesses one contribution, centred at *ca.* 576.5 eV, which is the Cr $2p_{3/2}$ peak, with its corresponding doublet (Cr $2p_{1/2}$) at *ca.* 586.2 eV. The binding energy value of Cr $2p_{3/2}$ is akin to that reported for chromium forming $Cr_2O_3$ (576.7–576.8 eV) [32], and the FWHM value from the Cr $2p_{3/2}$ signal is in all cases *ca.* 2.9 eV, which is very close to that of 3.03 eV as reported for bulky $Cr_2O_3$ [33]. The results confirm the formation of $Cr_2O_3$, as previously obtained from XRD measurements, and the absence of superficial Cr(VI). On the other hand, the XPS results corresponding to the sulfided samples reflect a shift of the Cr $2p_{3/2}$ binding energy to lower values (Table 2) after the sulfidation process at 400 °C

**Table 2**
Spectral parameters and surface atomic ratios of precursors and sulfided catalysts obtained by XPS analysis

| Sample | Binding energy (eV) | | S/Cr atomic ratio |
|---|---|---|---|
| | Cr $2p_{3/2}$<br>$Cr^{3+}$ | S $2p_{3/2}$<br>$Cr_xS_y$ | |
| Catalysts precursors | | | |
| AlSBACr-15 | 576.4 | – | – |
| AlSBACr-20 | 576.4 | – | – |
| AlSBACr-25 | 576.6 | – | – |
| AlSBACr-30 | 576.4 | – | – |
| Sulfided catalysts | | | |
| AlSBACr-15 | 575.4 | 162.1 | 0.44 |
| AlSBACr-20 | 575.7 | 161.5 | 0.10 |
| AlSBACr-25 | 575.6 | 161.4 | 0.27 |
| AlSBACr-30 | 575.9 | 161.4 | 0.39 |

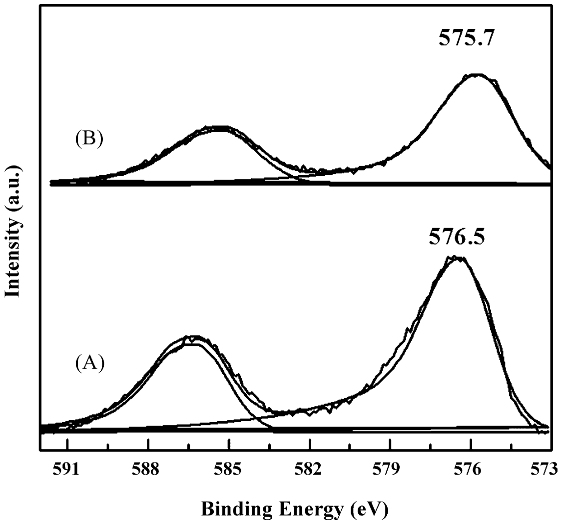

**Fig. 5.** Cr 2p core level spectra of AlSBACr-20 sample: (A) catalyst precursor and (B) sulfided catalyst.

(Fig. 5B). The Cr $2p_{3/2}$ signal is now centred at binding energy values lower than 576.0 eV, ranging from 575.4 to 575.9 eV. The BEs reported for $Cr_2S_3$ and CrS are 574.9 and 575.6 eV, respectively [32], therefore the Cr $2p_{3/2}$ BE determined for the sulfided samples are close to the value reported for CrS. Similarly, Gaspar et al. reported that the BE of the Cr $2p_{3/2}$ level of unsupported $Cr^{2+}$ species was of 575.5 eV [34]. Concerning the FWHM values of sulfided samples, they all show an increase up to a value close to 3.4 eV, and the authors [34] have pointed out that the observed increase of the FWHM is related to the coexistence of two different oxidation states that could be related to the coexistence of both $Cr^{2+}$ and $Cr^{3+}$ on the surface. All these results have led us to conclude that after the sulfidation process, only superficial chromium(II) sulfide is formed, while only a fraction of chromium(III) oxide remains located under the layer of CrS, which can be detected by the X-ray beam.

As far as the S 2p signal is concerned, that corresponding to the AlSBACr-30 sulfided catalyst is depicted in Fig. 6. The S 2p signal can be decomposed into two peaks ascribed to the S $2p_{3/2}$ and S $2p_{1/2}$ photoelectrons. The S $2p_{3/2}$ value is 161.5 eV, which is lower than that found for $Cr_2S_3$ (162.5 eV) and close to the value reported for $S^{2-}$ ions in CrS (161.0–161.7 eV). However, in the sample with the lower amount of chromium (AlSBACr-15), a value close to that of $Cr_2S_3$ is found.

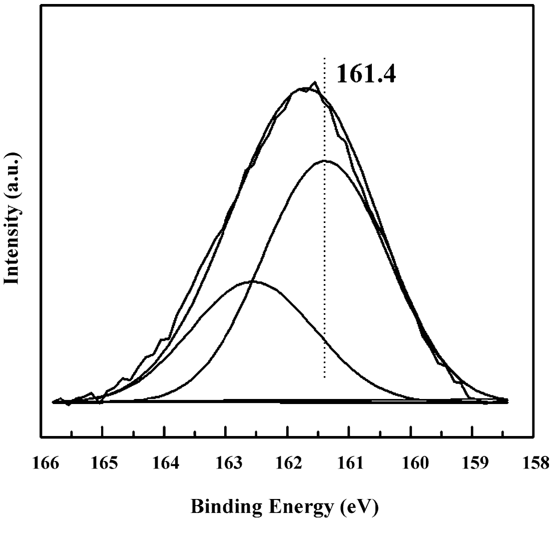

**Fig. 6.** S 2p core level spectra for AlSBACr-30 sulfided catalyst.

It has been reported that $Cr_2S_3$ is the most stable chromium sulfide formed after heating $Cr_2O_3$ in the presence of an $H_2/H_2S$ atmosphere [35]. Dumeignil et al. [13] have reported that first $Cr_2O_3$ gives $Cr_2S_3$ progressively through the formation of $CrS_x$ intermediates, to later be decomposed into CrS. These authors studied the formation of $Cr_2S_3$ as a function of the chromium loading and they found a higher percentage of $Cr_2S_3$ when the amount of chromium was lower. In the same way, the Cr $2p_{3/2}$ BE values of our sulfided samples (Table 2) tend, at lower chromium loadings, to be near to the typical value of $Cr_2S_3$ (574.9 eV). In the same way, the S $2p_{3/2}$ signal tends to be the typical value of sulfur forming such a compound. Moreover, the S/Cr atomic ratio is higher for AlSBACr-15 (Table 2). Accordingly, it could be thought that the decomposition of such a sulfide into CrS only takes place to a greater extent at higher chromium loading, i.e., in samples with $CrO_3$ loading higher than 15 wt.%. However, the authors have pointed out that for low Cr loadings the system is represented as a $CrS_x$ phase, while for higher loadings the systems could be thought of as a CrS phase, but supported on $Cr_2O_3$. As Cr electronegativity is higher than that of Al, in the sulfided supported on $Cr_2O_3$ some Cr–S bonds are likely to be weakened, provoking a higher number of labile S species which will be more active in the HDS reactions [12]. For this reason AlSBACr-20 is more active than AlSBACr-15. However, the ulterior increase in the $CrO_3$ loading leads to the formation of bigger particles of $Cr_2O_3$ with lower surface area, which produces a lower degree of sulfidation and lower activity.

In view of the above results, we can conclude that in the case of the sample with lower Cr amount, the $CrS_x$ formed interacts more strongly with the material support, thus decreasing the quantity of labile sulfur and therefore its catalytic performance (see catalytic study section). On the other hand the other three samples, with a greater amount of chromium, seem to confirm the formation of CrS supported on $Cr_2O_3$, thus increasing the amount of labile sulfur with the consequent improvement in the catalytic activity.

Quantitative XPS data show that for sulfided catalysts (Table 2) the S/Cr atomic ratio increases with the chromium content, except for the catalysts with the lower amount of chromium, which possess the highest value. The increase in the ratio is related to the higher degree of sulfurization at higher chromium content, although in no case does it reach the stoichiometric value of 1 when the CrS compound is formed. Only a superficial sulfurization could take place. Besides, this ratio is not related to the catalytic activity. With regard to this, the AlSBACr-15 sample, in spite of having the highest S/Cr atomic ratio, possesses the lowest catalytic activity. As will be stated in TPRS section, due to the higher interaction with the material support, most of the chromium sulfide acts as if it were bulk and less sulfur labile is formed on this sample.

### 3.2.5. $H_2$-TPRS

The $H_2$-TPRS patterns of sulfided chromium catalysts are shown in Fig. 7. It should be considered that the initial oxidation state of chromium in the catalyst precursors is +3, as seen from the XRD and XPS results. Besides, after the sulfidation process the sulfided chromium formed seems to be CrS, once the analysis of the XPS has been fully studied. By considering that the reduction of chromium sulfide to $Cr^0$ cannot occur, because it is thermodynamically unfavourable in the experimental conditions employed, the reduction of chromium sulfided catalysts cannot proceed further than CrS. Hence, the TCD signal in the TPR experiments should be only due to physisorbed $H_2S$ or recombination/hydrogenation of

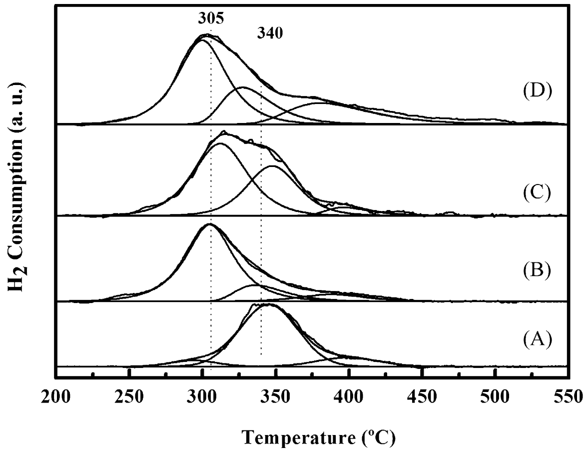

**Fig. 7.** $H_2S$-TPRS profiles of the sulfided catalysts: (A) AlSBACr-15, (B) AlSBACr-20, (C) AlSBACr-25 and (D) AlSBACr-30.

the S–H groups. Accordingly, it has been reported that the removal of the $H_2S$ excess adsorbed on the surface takes place at temperatures lower than 200 °C [36]. In no case is this peak observed, thus we discard the adsorption of $H_2S$ on the catalysts. In all cases, two main peaks are noticeable; the first one centred at *ca.* 300 °C which could be related with the desorption of labile-S in the form of $H_2S$, which has been reported as being the active site in the HDS reactions [29], so long as they are responsible of the formation of coordinatively unsaturated sites, as is fully documented in the literature [37]. The second peak is centred at 340 °C and is assigned to the $H_2S$ removed from bulk CrS. However the presence of a third small peak is noticeable which could be due to the reduction of Cr(III) to Cr(II) forming a sublayer under the chromium sulfide. This peak is almost negligible in the AlSBACr-15 catalyst with the lower chromium content, where a higher formation of hydrogen sulfide coming from bulk CrS is observed due to the stronger interaction of this sulfide with the support. On the other hand, the sample which shows a higher proportion of labile-S compared to that coming from the bulk is AlSBACr-20, and has shown better catalytic activity, so confirming the role of this type of sulfur in the HDS reactions. The samples with the highest chromium loading have a lower proportion of labile-S/bulk, which implies a lower catalytic activity. The main conclusion to be taken from these results is that there is an optimum quantity of metallic loading, where the amount of labile sulfur formed is sufficient to obtain good catalytic results.

## 4. Conclusions

Chromium sulfided based catalysts supported on an aluminium doped SBA-15 show good activities in the DBT hydrodesulfurization at high-pressure of hydrogen. The hydrogenation selectivity of these chromium containing catalysts is higher than direct desulfurization selectivity for all catalysts in all range of studied temperature. Sample AlSBACr-20 showed the best catalytic performance which was related to the amount of labile sulfur as determined by $H_2$-TPRS. A catalyst with a similar amount of chromium supported on a pure siliceous SBA-15 shows a low activity, indicating that the incorporation of Al modifies the acidic properties favouring so the formation of labile sulfur which improves the catalytic performance of these catalysts with regards to that using SBA-15 without aluminium as material support.

## Acknowledgements

We gratefully acknowledge the Ministerio de Educación y Ciencia (Project MAT2003-02986 and MAT2006-02465). M.G.C. also thanks Ministerio de Educación y Ciencia (Spain) for a fellowship. A.I.M. is also grateful to Junta Andalucía for a postdoctorate contract (Excellence Proyect P06-FQM-01661).

## References

[1] J.C. Plumail, in: Proceedings of the ARTC Seventh Annual Meeting Incorporation the ARTC, Singapore, 2004.
[2] E. Benazzi, C. Cameron, in: HART (Eds.), World Diesel Clean Technology, World Diesel Report, 2005, pp. 6–11.
[3] M. Egorova, R. Prins, Competitive hydrodesulfurization of 4,6-dimethyldibenzothiophene, hydrodenitrogenation of 2-methylpyridine, and hydrogenation of naphthalene over sulfided NiMo/$\gamma$-$Al_2O_3$, J. Catal. 224 (2004) 278–287.
[4] C. Song, X. Ma, New design approaches to ultra-clean diesel fuels by deep desulfurization and deep dearomatization, Appl. Catal. B 41 (2003) 207–238.
[5] M. Breysse, P. Afanasiev, C. Geantet, M. Vrinat, Overview of support effects in hydrotreating catalysts, Catal. Today 86 (2003) 5–16.
[6] T. Kabe, A. Ishihara, W. Qian, Hydrodesulfurization and Hydrodenitrogenation, Wiley-VCH, Kodansha/Tokyo/New York, 1999.
[7] T. Kabe, A. Ishihara, W. Qian, A. Funato, T. Kawano, Elucidation of sulfur mobility on Cr, Mo and W-based catalysts in hydrodesulfurization using a$^{35}$S pulse tracer method, React. Kinet. Catal. Lett. 68 (1999) 69–75.
[8] C.S. Brooks, Thiophene hydrodesulfurization over transition metal zeolites, Surf. Tech. 10 (1980) 379–397.
[9] M.J. Ledoux, O. Michaux, G. Agostini, The influence of sulfide structures on the hydrodesulfurization activity of carbon-supported catalysts, J. Catal. 102 (1986) 275–288.
[10] M. Sychev, V.H.J. De Beer, A. Kodentrov, E.M. Van Oers, R.A. Van Santen, Chromia- and chromium sulfide-pillared clays: preparation, characterization, and catalytic activity for thiophene hydrodesulfurization, J. Catal. 168 (1997) 245–254.
[11] F.J. Pérez-Reina, E. Rodríguez-Castellón, A. Jiménez-López, Chromia-pillared $\alpha$-zirconium phosphate materials as catalysts for thiophene hydrodesulfurization, Langmuir 15 (1999) 2047–2054.
[12] W. Qian, T. Kawano, A. Funato, A. Ishihara, T. Kabe, Hydrodesulfurization and hydrogenation of radioactive $^{35}$S-labeled dibenzothiophene on alumina-supported chromium and promoted chromium catalysts, Phys. Chem. Chem. Phys. 3 (2001) 261–266.
[13] F. Dumeignil, H. Amano, D. Wang, E.W. Qian, A. Ishihara, T. Kabe, Study of the sulfidation process of $CrO_3$–$Al_2O_3$ hydrodesulfurization catalysts by a $^{35}$S-labeled $H_2S$ pulse tracer method, Appl. Catal. A 249 (2003) 255–263.
[14] S. Myllyoja, J. Räty, T.A. Pakkanen, Catalytic activity of Cr/Co alumina catalysts in thiophene hydrodesulfurization, J. Mol. Catal. A 157 (2000) 245–252.
[15] G. Murali Dhar, B.N. Srinivas, M.S. Rana, M. Kumar, S.K. Maity, Mixed oxide supported hydrodesulphurization catalysts—a review, Catal. Today 86 (2003) 45–60.
[16] H. Topsoe, B.S. Clausen, F.E. Massoth, Hydrotreating catalysts, in: J.R. Anderson, M. Boudart (Eds.), Catalysis Science and Technology, vol. 11, Springer, Berlin, 1996, pp. 1–310.
[17] R.R. Chianelli, M. Daage, M.J. Ledoux, Fundamental studies of transition-metal sulfide catalytic materials, Adv. Catal. 40 (1994) 177–232.
[18] A. Wang, Y. Wang, T. Kabe, Y. Chen, A. Ishihara, W. Qian, P. Yao, Hydrodesulfurization of dibenzotiophene over siliceous MCM-41-supported catalysts. II. Sulfided Ni–Mo catalysts, J. Catal. 210 (2002) 319–327.
[19] A. Wang, Y. Wang, T. Kabe, Y. Chen, A. Ishihara, W. Qian, Hydrodesulfurization of dibenzotiophene over siliceous MCM-41-supported catalysts. I. Sulfided Co–Mo catalysts, J. Catal. 199 (2001) 19–29.
[20] T. Chiranjeevi, P. Kumar, M.S. Rana, G. Murali Dhar, T.S.R. Prasada Rao, Physico-chemical characterization and catalysis on mesoporous Al-HMS supported molybdenum hydrotreating catalysts, J. Mol. Catal. A 181 (2002) 109–117.
[21] T. Halachev, R. Nava, L. Dimitrov, Catalytic activity of (P)NiMo/Ti-HMS and (P)NiW/Ti-HMS catalysts in the hydrogenation of naphtalene, Appl. Catal. A 169 (1998) 111–117.
[22] G. Murali Dhar, G. Muthu Kumaran, M. Kumar, K.S. Rawat, L.D. Sharma, B. David Raju, K.S. Rama Rao, Physico-chemical characterization and catalysis on SBA-15 supported molybdenum hydrotreating catalysts, Catal. Today 99 (2005) 309–314.
[23] G. Muthu Kumaran, Shelu Garg, Kapil Soni, Manoj Kumar, L.D. Sharma, G. Murali Dhar, K.S. Rama Rao, Effect of Al-SBA-15 support on catalytic functionalities of hydrotreating catalysts. I. Effect of variation of Si/Al ratio on catalytic functionalities, Appl. Catal. A 305 (2006) 123–129.
[24] O.Y. Gutiérrez, G.A. Fuentes, C. Salcedo, T. Klimova, SBA-15 supports modified by Ti and Zr grafting for NiMo hydrodesulfurization catalysts, Catal. Today 116 (2006) 485–497.
[25] L. Kaluza, M. Zdrazil, N. Zilkova, J. Cejka, High activity of highly loaded $MoS_2$ hydrodesulfurization catalysts supported on organised mesoporous alumina, Catal. Commun. 3 (2002) 151–157.
[26] L. Vradman, M.V. Landau, M. Herskowitz, V. Ezersky, M. Talianker, S. Nikitendo, Y. Koltypin, A. Gedanken, High loading of short WS2 slabs inside SBA-15: promotion with nickel and performance in hydrodesulfurization and hydrogenation, J. Catal. 213 (2003) 163–175.
[27] M. Gómez Cazalilla, J.M. Mérida Robles, A. Gurbani, E. Rodríguez Castellón, A. Jiménez López, Characterization and acidic properties of Al-SBA-15 materials prepared by post-synthesis alumination of a low cost ordered mesoporous silica, J. Solid State Chem. 180 (2007) 1130–1140.

[28] H. McMurdie, M. Morris, E. Evans, B. Paertzkin, W. Ng-Wong, Y. Zhang, C.R. Hubbard, Standard X-ray diffraction powder patterns from the JCPDS research associateship, Power Diffr. 2 (1987) 41–52.

[29] F. Dumeignil, K. Sato, M. Imamura, N. Matsubayashi, E. Payen, H. Shimada, Characterization and hydrodesulfurization activity of CoMo catalysts supported on sol–gel prepared $Al_2O_3$, Appl. Catal. A 287 (2005) 135–145.

[30] A. Infantes-Molina, J. Mérida-Robles, E. Rodríguez-Castellón, J.L.G. Fierro, A. Jiménez-López, Effect of molybdenum and tungsten on Co/MSU as hydrogenation catalysts, J. Catal. 240 (2006) 258–267.

[31] L. Zhang, Y. Zao, H. Dai, H. He, C.T. Au, A comparative investigation on the properties of Cr-SBA-15 and CrOx/SBA-15, Catal. Today 131 (2008) 42–54.

[32] J.F. Moulder, W.F. Stickle, P.E. Sool, K.D. Bomber, Handbook of X-Ray Photoelectron Spectroscopy, PerkinElmer, Eden Prairie, MN, 1992.

[33] B. Liu, M. Terano, Investigation of the physico-chemical state and aggregation mechanism of surface Cr species on a Phillips CrOx/$SiO_2$ catalyst by XPS and EPMA, J. Mol. Catal. A 172 (2001) 227–240.

[34] A.B. Gaspar, C.A.C. Perez, L.C. Dieguez, Characterization of Cr/$SiO_2$ catalysts and ethylene polymerization by XPS, Appl. Surf. Sci. 252 (2005) 939–949.

[35] T.A. Pecoraro, R.R. Chianelli, Hydrodesulfurization catalysis by transition metal sulfides, J. Catal. 67 (1981) 430–445.

[36] P.J. Mangnus, A. Riezebos, A.D. van Langeveld, J.A. Moulijn, Temperature-programmed reduction and HDS activity of sulfided transition metal catalysts: formation of nonstoichiometric sulfur, J. Catal. 151 (1995) 178–191.

[37] P. Afanasiev, On the interpretation of temperature programmed reduction patterns of transition metals sulphides, Appl. Catal. A 303 (2006) 110–115.